

Contents lists available at [SciVerse ScienceDirect](http://SciVerse.Sciencedirect.com)

European Polymer Journal

journal homepage: www.elsevier.com/locate/europolj

Macromolecular Nanotechnology

Quantitative estimation of the strength of specific interactions in polyurethane elastomers, and their effect on structure and properties

Kristóf Bagdi^{a,b}, Kinga Molnár^{a,b}, Mihály Kállay^c, Peter Schön^d, Julius G. Vancsó^{d,*}, Béla Pukánszky^{a,b}^a *Laboratory of Plastics and Rubber Technology, Department of Physical Chemistry and Materials Science, Budapest University of Technology and Economics, H-1521 Budapest, P.O. Box 91, Hungary*^b *Institute of Materials Science and Environmental Chemistry, Chemical Research Center, Hungarian Academy of Sciences, H-1525 Budapest, P.O. Box 17, Hungary*^c *Laboratory of Physical Chemistry, Department of Physical Chemistry and Materials Science, Budapest University of Technology and Economics, H-1521 Budapest, P.O. Box 91, Hungary*^d *Materials Science and Technology of Polymers, MESA⁺ Institute for Nanotechnology, University of Twente, Enschede NL-7500, The Netherlands*

ARTICLE INFO

Article history:

Received 8 July 2012

Accepted 22 July 2012

Available online 1 August 2012

Keywords:

Polyurethane elastomer

Stoichiometry

Specific interactions

Phase separation

Physical cross-links

Structure-property correlations

ABSTRACT

Two sets of segmented polyurethane (PU) elastomers were prepared from crystalline MDI, butanediol and a polyester or a polyether polyol, respectively. The molar mass of both polyols was 1000 g/mol. The –OH functional group ratio of polyol/total diol was kept constant at a value of 0.4, while the ratio of the isocyanate and hydroxyl groups (NCO/OH) changed between 0.90 and 1.15 in the polyester, and 0.94 and 1.15 in the polyether polyurethanes, respectively. One step bulk polymerization was carried out in an internal mixer and the samples were compression molded for testing. Advanced molecular modeling was used to estimate the strength of various specific interactions quantitatively in the polymers studied. Fifteen different specific interactions were identified in polyester while thirteen in polyether PU considering only hydrogen bonds. Estimated binding enthalpy changes between 11 and 26 kJ/mol. The results proved that hard–soft and not hard–hard segment interactions control phase separation of linear segmented polyurethanes. A new model was developed to quantify the relative importance of specific interactions acting between the two types of segments. The calculations predicted better solubility of the soft phase in hard domains in polyester than in polyether polyurethanes. Besides the mutual solubility of the phases, their size and mechanical properties also depend on these interactions shown by the study of phase structure using a novel combination of various methods in a wide length scale. Properties are determined by different aspects of morphology. Transparency depends on the amount of ordered hard phase, stiffness and hardness on phase composition, while ultimate properties on stoichiometry, which determines molecular weight and the number of physical cross-link points.

© 2012 Elsevier Ltd. All rights reserved.

1. Introduction

Polyurethane chemistry opened the way to a new class of high performance materials such as coatings, adhesives, elastomers, fibers and foams. Based on a simple

polyaddition reaction, polyurethanes proved to be very versatile polymers [1]. Important group of these materials, the polyurethane elastomers, are widely used engineering materials and are well known for their outstanding mechanical, thermal, and adhesive properties [2]. They consist of an alternating flexible component or macrodiol, called soft segment, and a stiff component derived from diisocyanate and a chain extender, called hard segment [3]. The interactions between hard segments containing

* Corresponding author. Tel.: +31 (0)53 489 2974; fax: +31 (0)53 489 3823.

E-mail address: G.J.Vancso@utwente.nl (J.G. Vancsó).

many hydrogen bonds and dipole–dipole interactions provide a pseudo-crosslinked network structure between linear polyurethane chains [4].

Because of their advantageous properties like haemo and tissue compatibility segmented linear polyurethanes are extensively used in health care mostly as medical devices [5,6]. They are applied as encapsulants for hollow-fiber devices, dip-molded gloves and balloons, asymmetric membranes, functional coatings, and as extruded profiles for catheters [7–9]. Endovascular treatment of aneurisms and arteriovenous malformations also provide, for example, a promising area in the biomedical field [10,11]. However, composition, phase separation and thus structure must be adjusted to satisfy the stringent conditions of medical applications.

Degradation studies on the implanted polyurethane elastomers resulted in the progressive development of soft segments from the polyester to polyether [12] and later to polycarbonate [13] and poly(dimethylsiloxane) [14] macroradiols. These changes made the implants more resistant against hydrolytic and oxidative degradation [15]. Recently the preparation of poly(isobutylene)-diol based aromatic polyurethanes were reported; the polymers proved to have excellent degradation stability [16]. On the other hand, carcinogenic and mutagenic aromatic diamines (methylenedianiline and toluidenedianiline) have been identified as degradation products forming from polyurethanes containing aromatic diisocyanates; however, the question whether the concentration of these harmful degradation products attain physiologically relevant levels is currently unresolved and strongly debated [17].

The role of interactions and especially that of hydrogen bonds on structure development has been extensively studied previously [18–24]. The critical role of hydrogen bonds in phase separation was shown, for example, by MacKnight et al. [19–21] in several papers. Nonpolar polyols capable of only dispersion interaction phase separated practically completely in the polyurethanes prepared [19]. Apparently the interaction of the soft and hard segments determines the extent of phase separation, the structure formed and thus the properties of the polymer [25,26]. This consideration is strongly supported by the results of Bras et al. [27], who showed that phase separation of the hard and soft segments happens before hydrogen bonding of the hard segments takes place. Apart from experimental investigations, theoretical studies on the interactions influencing the structure of PU polymers are rather scarce. Previous theoretical studies employed low-level semi-empirical models [28] or density functional (DFT) methods using functionals and basis sets which provide poor results for weak interactions [29]. Another common feature of the aforementioned studies is that only a limited number of interactions were investigated, and no attempt was made to map all the dominant interactions between polymer chains, like the effect of chain-end groups, which can play a significant role for shorter chains. Moreover, according to our knowledge, apart from studying pair interactions, no attempt was made to take into consideration composition, i.e. the number of interacting groups, in the determination of the effect of interactions on structure and properties.

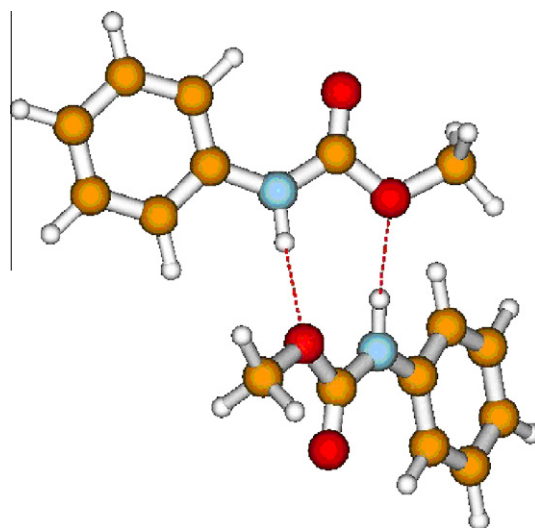
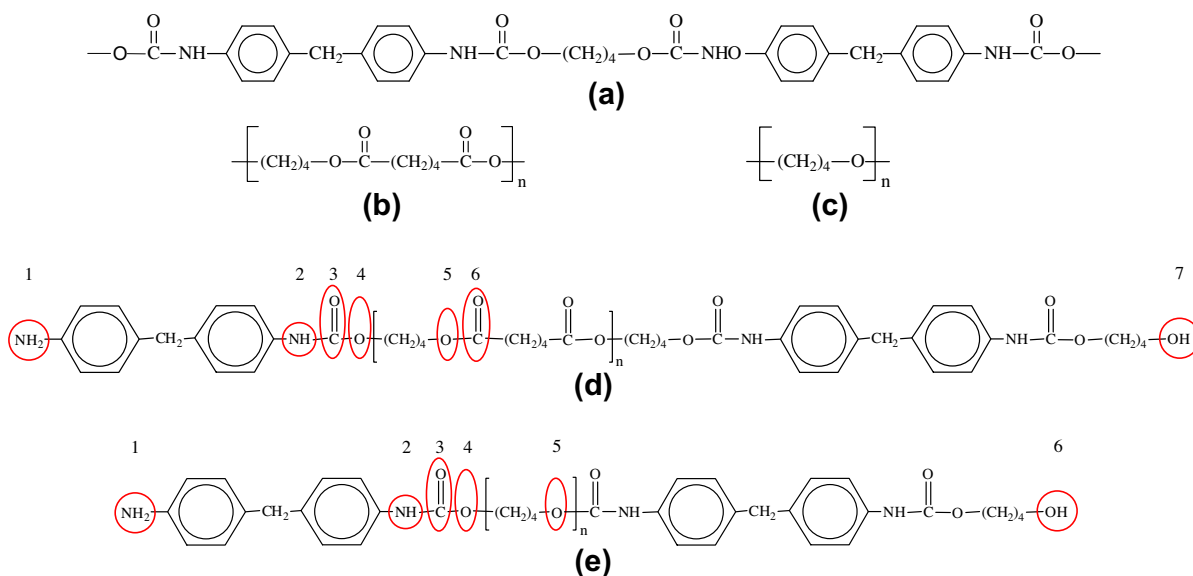


Fig. 1. Modeling of the interaction between two urethane groups. Interaction between the >HN and >O groups; binding enthalpy is 22 kJ/mol.

Phase separation leads to the formation of a hierarchical structure with units of various forms and sizes [30–33]. Besides a crystalline or at least highly ordered phase, soft and hard segments form corresponding phases, which are partially soluble in each other [34–37]. Many attempts have been made to characterize interactions and structure in segmented polyurethanes. Mainly Fourier transform infrared spectroscopy (FTIR) is used for the characterization of the hydrogen bonds forming [38–40], but the interaction of only a few of the interacting pairs can be studied with this method. A wide range of techniques are applied for the characterization of structure including X-ray diffraction [41,42], small angle X-ray scattering [43,44], light scattering [45], transmission electron microscopy [46,47] and atomic force microscopy [48,49]. However, most studies focus on one or maybe on a few of these techniques, and they rarely cover a wide length scale from the nanometer to the micrometer [32]. Even scarcer are papers which successfully relate interactions to structure and properties. Although Ginzburg et al. [50] succeeded in finding correlation between the composition (hard segment chemical structure, hard segment weight fraction, soft segment equivalent weight) and the Young's modulus of segmented polyurethanes, practically no relationship have been published yet for other characteristics like transparency or tensile properties.

The goal of this communication is to discuss the possible effect of specific interactions on the structure and properties of segmented linear polyurethane elastomers. Two series of samples were prepared from a polyether and a polyester polyol with similar molecular weights. The structure of the polymers was characterized by several methods covering a wide length scale. Advanced molecular model calculations were carried out to identify all the dominant interactions and to estimate their strength. A unique model was created to take into account the role of composition, i.e. the number of interacting species, in structure



Scheme 1. Molecular structure of the polyurethanes studied. (a) hard segment (b) polyester soft segment (c) polyether soft segment (d) polyester PU (e) polyether PU.

formation. An attempt was also made to relate interactions to structure and properties.

2. Experimental

4,4'-Methylenebis(phenyl isocyanate) (MDI, Aldrich, 98%) was used as isocyanate and 1,4-butanediol (BDO, Aldrich, 99%) as chain extender in both series. The polyether polyol was polytetrahydrofuran (Terathane 1000), while the polyester was diol-end-capped poly(1,4-butylene adipate). Both polyols had a molar mass of 1000 g/mol and were acquired from Aldrich. MDI was used as received, BDO was distilled at 190 °C under vacuum, and the polyols were dried at 80 °C under vacuum for 24 h prior to the reaction. The -OH functional group ratio of polyol/total diol was kept constant at 0.4 in all experiments. The variable was the ratio of the isocyanate and hydroxyl groups (NCO/OH ratio), which changed between 0.90 and 1.15 in the polyester and 0.94 and 1.15 in the polyether polyurethanes. One step bulk polymerization was carried out in an internal mixer (Brabender W 50 EH) at 150 °C, 50 rpm for 30 min. The polymer was compression molded into 1 mm plates at 200 °C and 5 min using a Fontijne SRA 100 machine then cooled down in 10 min to room temperature by cooling the plates of the mold with running water. Cooling conditions were the same in each case thus the kinetics of phase separation was influenced only by composition and the changing molecular weight of the polymer; we considered this effect to be small.

The torque and temperature of mixing were recorded during polymerization. The time dependence of these quantities offers information about the kinetics of polymerization and the molecular weight of the final product. Fourier transform attenuated total reflectance infrared spectra (FTIR-ATR) were recorded on the compression

molded plates in the wavelength range of 4000 and 400 cm^{-1} , using a Varian Scimitar 2000 apparatus equipped with a Specac Golden Gate ATR reflection unit and a wide band MCT detector. The original spectra were corrected before evaluation using the Advanced ATR Correction Algorithm developed by Thermo Scientific [51]. The relaxation transitions of the polymers were studied by differential scanning calorimetry (DSC) and dynamic mechanical analysis (DMA). Two heating and a cooling run were performed in N_2 atmosphere between -120 and 250 °C on 10 mg samples with a rate of 20 °C/min using a Mettler Toledo TA 4000 apparatus equipped with a DSC 30 cell. DMA spectra were recorded on samples with $20 \times 6 \times 1$ mm dimensions between -120 and 200 °C at 2 °C/min heating rate in N_2 atmosphere using a Perkin Elmer Pyris Diamond DMA apparatus. The measurements were carried out in tensile mode at 1 Hz frequency and 10 μm deformation. The structure of the samples was characterized by wide (WAXS) and small angle (SAXS) X-ray diffraction (XRD). WAXS patterns were recorded using a Phillips PW 1830/PW 1050 equipment with $\text{CuK}\alpha$ radiation at 40 kV and 35 mA in reflection mode. For the recording of the SAXS patterns a compact Kratky-type camera was used with an M-Braun one-dimensional position sensitive proportional counter having a channel width of about 52 μm . The distance between the sample and the detector was 20 cm. The X-ray source was a Cu anode sealed X-ray tube equipped with a Ni filter to suppress the $\text{K}\beta$ line. The beam used was line focused, its dimensions being 16 mm horizontally and 0.2 mm vertically. The morphology of smooth, cross-sectioned areas of selected samples was examined by AFM. The measurements were done in air under ambient conditions using a Multimode AFM with a NanoScope V controller and NanoScope version 7.30 software (Bruker/Digital Instruments, Santa Barbara, CA).

Table 1

The strength of hydrogen bonding interaction complexes developing in polyester polyurethanes and their contribution to enthalpy in a unit mass of polymer at different stoichiometries. See the identification of interacting groups in Scheme 1b.

Type of interaction between various groups	Binding enthalpy (kJ/mol)			Bond length (Å)	Contribution to enthalpy decrease (J/g) for NCO/OH ratio of		
					0.94	1.00	1.15
NH–CO(<i>est</i>)	2	6	26	1.98	51.7	52.3	48.5
NH ₂ –CO(<i>est</i>)	1	6	22	2.18	–	0.2	7.8
NH–OH	2	7	22	1.8	0	0	–
NH–CO(<i>ur</i>)	2	3	22	1.97	6.3	7.3	7.4
CO(<i>ur</i>)–OH	3	7	22	1.93	3.7	0.3	–
NH–O(<i>ur</i>)	2	4	22	2.04	6.7	7.3	7.5
NH ₂ –NH	1	2	19	2.08	–	0	0
HO–OH	7	7	18	1.94	0	0	–
NH–O(<i>est</i>)	2	5	18	2.13	2.3	2.4	2.4
NH ₂ –OH	1	7	16	2.02	–	0	–
NH ₂ –CO(<i>ur</i>)	1	3	16	2.09	–	0	0.5
NH ₂ –OH	1	7	15	2.06	–	0	–
CO(<i>est</i>)–OH	6	7	14	1.99	0.1	0	–
NH ₂ –O(<i>est</i>)	1	5	12	2.98	–	0	0.1
NH ₂ –NH ₂	1	1	11	2.36	–	0	0

Tapping Mode AFM was operated utilizing cantilever vibration free amplitude of 1.5 V in air. Imaging was performed at 0.5–1 Hz scan rates. Mechanical properties were determined by tensile testing on dog-bone type specimens with 50 × 10 × 1 mm dimensions at 100 mm/min cross-head speed using an Instron 5566 apparatus. Tensile strength and elongation-at-break were derived from recorded force vs. elongation traces, while tensile modulus was determined from the initial, linear section of the traces. Shore A hardness was measured on 4 mm thick samples created by the stacking of 1 mm pieces. The transparency of the compression molded plates was determined using a Spekol UV–VIS apparatus at 500 nm wavelength.

3. Computational details

We carried out molecular modeling to map possible interactions among segments and to estimate their strength. To reduce the necessary time and computer capacity to a reasonable level, we selected small model compounds representing the characteristic groups. The ether bond was modeled by dimethyl ether, the ester group by methyl acetate, phenyl-N-methylcarbamate modeled the urethane group, while ethanol and aniline the chain-end –OH and –NH₂ groups. We assumed that at isocyanate excess the chain-end isocyanate groups transform to amines. The assumption was justified by FTIR analysis. We focused only on specific interactions, i.e. hydrogen bonds, and neglected dispersion interactions in the analysis.

During our calculations, the model systems were constructed first on the basis of chemical intuition. The geometry of the complexes was optimized subsequently. The torsional angle around the hydrogen bond was systematically changed by 60 degree increments in order to search for further possible stable hydrogen-bonded conformers. The geometry of each sterically allowed conformation was again optimized. In the cases where more than one stable conformer was found the one with the lowest energy was considered in subsequent calculations. For model

systems with more than one relevant functional group the above analysis was performed for each group, e.g., both the carbonyl and the ether oxygen atoms were considered for the methyl acetate-ethanol complex.

All the geometry optimizations for model systems were performed at the density functional theory (DFT) level using the MPW1B95 (modified Perdew and Wang exchange and Becke's 1995 correlation) functional [52] as well as the 6-31++G** basis set [53]. The MPW1B95 functional was designed for weak interactions, and it has been demonstrated in benchmark calculations that, for weak hydrogen-bonded complexes, the functional provides results close to the more elaborate second-order Møller-Plesset (MP2) method, while more recognized functionals, such as B3LYP (Becke 3-parameter Lee–Yang–Parr exchange–correlation functional), may exhibit poor performance and give qualitatively incorrect results [52,54]. To test the performance of the MPW1B95 functional for the studied systems, the binding energy of the hydrogen-bonded ethanol dimer was also computed by MP2 with the applied basis set. The error of DFT for the strength of the hydrogen bond with respect to MP2, was 2.3 kJ/mol, which seems to be reasonable. Basis set superposition error (BSSE) corrections might have also been considered [55,56]. However, we must call the attention to the fact here that based on benchmark calculations the developers of the DFT functional used by us concluded that BSSE corrections do not improve the agreement with high-level ab initio calculations or experimental results [52]. Accordingly we did not consider this correction in our study. Total energies were converted to enthalpies using the calculated rotational constants and harmonic vibrational frequencies via the standard formulas of statistical thermodynamics. The calculations were carried out by the Gaussian 03 suite of quantum chemical programs [57].

4. Results and discussion

The calculation of interactions and their respective values for the two types of polymers are discussed first. Their

Table 2

The strength of hydrogen bonding interaction complexes developing in polyether polyurethanes and their contribution to enthalpy in a unit mass of polymer at different stoichiometries. See the identification of interacting groups in Scheme 1a.

Type of interaction between various groups	Binding enthalpy (kJ/mol)			Bond length (Å)	Contribution to enthalpy decrease (J/g) for NCO/OH ratio of		
					0.94	1.00	1.15
<i>NH–O(eth)</i>	2	5	24	1.94	48.0	48.8	41.7
CO–OH	3	6	22	1.93	1.9	0.1	–
<i>NH–CO</i>	2	3	22	1.97	8.4	9.3	6.2
NH–OH	2	6	22	1.80	0	0	–
<i>NH–O(ur)</i>	2	4	22	2.04	8.7	9.3	6.9
O(eth)–OH	5	6	20	1.92	1.8	0.1	–
NH ₂ –NH	1	2	19	2.08	–	0	0
OH–OH	6	6	18	1.94	0	0	–
NH ₂ –OH	1	6	16	2.02	–	0	0
NH ₂ –CO	1	3	16	2.09	–	0.1	3.5
NH ₂ –OH	1	6	15	2.06	–	0	–
NH ₂ –O(eth)	1	5	13	2.07	–	0.1	2.4
NH ₂ –NH ₂	1	1	11	2.36	–	0	0

influence on relaxation transitions, structure and properties are analyzed in subsequent sections. Finally the relationships between interaction, structure and properties, as well as consequences for practice are discussed at the end of the paper.

4.1. Interactions, phase separation

First we identified the stable hydrogen-bonded complexes of the model compounds and computed the corresponding binding enthalpies. A possible interaction forming between the urethane groups of adjacent molecules is demonstrated in Fig. 1. The rest of the interacting pairs are shown in Figs. S1 and S2 of the Supporting information. The binding enthalpy between the >NH and the >O group is 22 kJ/mol in the presented case. However, urethane groups can enter into another interaction with each other; the enthalpy of binding between the >NH and the >CO carbonyl oxygen is also estimated as 22 kJ/mol. The chemical structures of the hard and soft segments as well as the polyester and polyether polyurethanes are shown in Scheme 1. The numbers in the Scheme 1d and e indicate groups interacting with each other. We identified fifteen specific interactions in the polyester and thirteen in the polyether polyurethane.

In further analysis we developed a novel model to quantify the relative importance of the particular interactions acting between hard (MDI–BDO–MDI) and soft (polyol) segments. Although pair interactions of segments have been considered before, according to our knowledge such a model taking into account composition and the number interaction species has never been published yet. We assumed that functional groups behave as individual molecules and react with each other to form hydrogen-bonded complexes in multiple equilibrium reactions. The mixture of the molecules and the complexes was considered to be ideal. The equilibrium constants of the reactions leading to complex formation were determined on the basis of the well-known relationship between equilibrium constants and the Gibbs free energy of reactions. The latter quantity was approximated by the negative value of the computed binding enthalpies for the corresponding hydrogen bonds.

The initial concentration of the molecules representing the functional groups was calculated from the amount of the starting materials. Using the equilibrium constants and initial concentrations, the non-linear system of equations was solved numerically for the multiple equilibrium reactions to obtain the equilibrium concentrations of hydrogen-bonded complexes. The latter values were used to characterize the strength of the corresponding hydrogen bonding enthalpy for the different pairs of interacting segments.

The interacting complexes, the identification of the interacting groups, the corresponding binding enthalpies, the bond lengths of the hydrogen bonds, as well as the enthalpy decrease of the polymer due to the hydrogen bonds are listed in Table 1 for the polyether polyurethane and in Table 2 for the polyester polymer at three different stoichiometric ratios. The interacting complexes and their enthalpy contributions are different at different stoichiometric ratios for obvious reasons. A polymer prepared at –OH excess does not contain a chain-end amine group and vice versa, we do not have –OH groups at isocyanate excess. The most important complexes dominating interactions in the material are indicated by *italics* in the two tables.

The driving force of phase separation consists of entropic and enthalpic contributions. In the Flory–Huggins model the entropy of mixing depends on the volume fraction of components, their molar volumes and on their degree of polymerization [58,59]. Assuming two polymers with a molecular mass of 40,000 g/mol consisting of repeat units with a molecular mass of 100 g/mol, the entropy contribution to the change of free enthalpy is less than 0.1 J/g. Considering the fact that this value decreases further in the case of block copolymers due to the restriction of the position of the A–B covalent bonds between the domains, restricted volume, and the perturbation of chain dimensions or elasticity entropy [60], we can state with quite large certainty that the entropy of mixing can be neglected in further considerations. This assumption was further confirmed by the calculation of the total enthalpy of interactions and their magnitude.

Table 3

Total binding enthalpies due to hard–hard and hard–soft segment interactions in the two types of polyurethanes calculated for the stoichiometric composition (NCO/OH ratio) of 1.

Type of polyurethane	Enthalpy decrease due to segmental interactions (J/g)	
	HS–SS	HS–HS
Polyester	54.7	14.6
Polyether	48.8	18.6

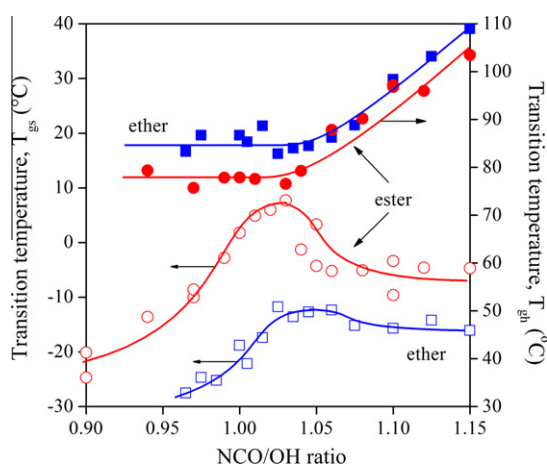


Fig. 2. Effect of polyol type and stoichiometry on the transition temperature of the phases. T_g was determined from $tg \delta$ traces (DMA); polyester PU soft (\circ) and (\bullet) hard phase, polyether PU (\square) soft and (\blacksquare) hard phase.

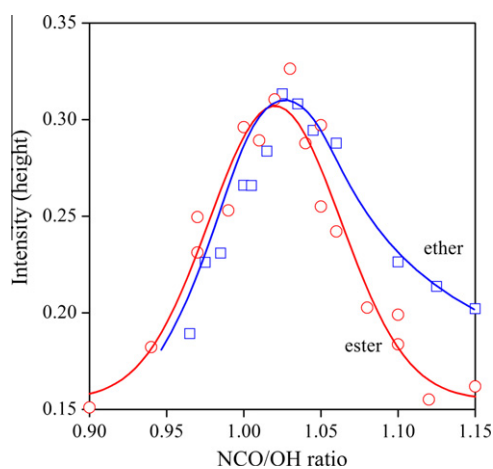


Fig. 3. Effect of polyol type and composition on the amount of relaxing soft segments ($tg \delta$, DMA) in polyurethane elastomers; (\circ) polyester, (\square) polyether PU.

In further analysis we considered the interaction of soft and hard segments. The interactions of Tables 1 and 2 can be divided into two main groups, i.e. to hard–hard (HS–HS) and hard–soft (HS–SS) segment interactions. Summarizing all the binding enthalpies of the corresponding groups allows us to estimate the total interaction enthalpy determining phase miscibility. Total interaction enthalpies of

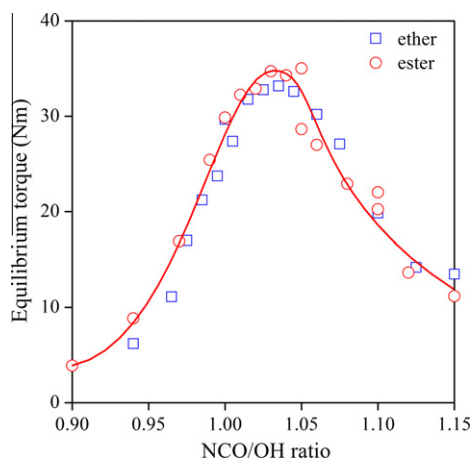


Fig. 4. Independence of the melt viscosity (equilibrium torque) of polyurethane elastomers of the type of polyol used. Effect of stoichiometry; (\circ) polyester, (\square) polyether PU.

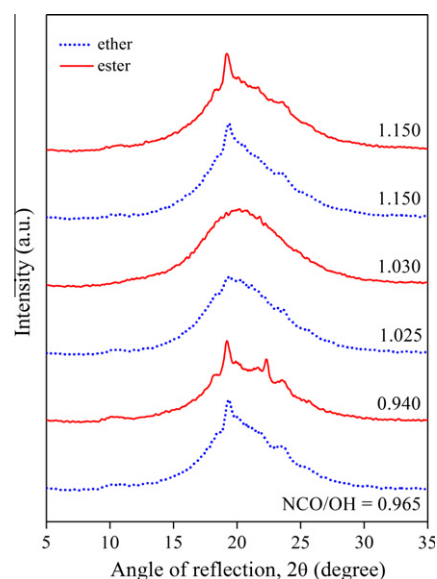


Fig. 5. XRD traces of selected polyurethane elastomers; effect of polyol type and stoichiometry on structure; polyether, --- polyester polyol. The numbers on the traces indicate the NCO/OH ratio.

the segments are listed in Table 3. Hard–soft interactions dominate in both polymers, but the relative ratio of HS–SS/HS–HS interactions is smaller for the polyether than for the polyester polyurethane. The total enthalpy decrease due to hard–soft bonds is almost four times larger than that of hard–hard interactions in the polyester PU, while somewhat more than twice as large in the polyether polymer. This conclusion is in line and it is strongly supported by earlier observations [25,26] and the results of Bras et al. [27] indicating that in segmented polyurethanes, phase separation is not driven by hydrogen bonding, but by the interaction of soft and hard segments. The difference observed between polyester and polyether urethanes is expected to lead to dissimilar phase separation and morphology in the two types of polyurethanes.

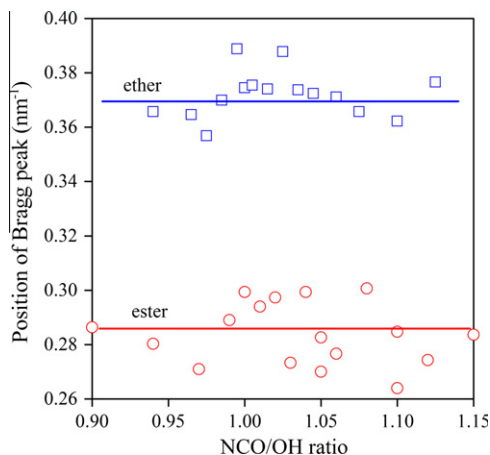


Fig. 6. Location of the scattering peak (q) in the SAXS traces plotted against the NCO/OH ratio. Effect of the polyol used; (○) polyester, (□) polyether PU.

4.2. Relaxation transitions

Dissimilar interactions of soft and hard segments should result in different relaxation behavior in the two polymers. The analysis of transition temperatures and the intensity of the transitions offer valuable information on the number of relaxing units and their mobility. Both DSC and DMA traces were recorded on all samples. Primary traces can be found in the [Supporting information](#) (Figs. S3–S6). The two techniques offer similar information on relaxation transitions, but the melting of the ordered hard phase also appears and can be studied on DSC traces. In [Fig. 2](#) we present the transition temperatures of the soft and hard phases derived from the temperature dependence of loss tangent determined by DMA. The maximum in the transition temperature of the soft phase was explained earlier by the rejection of soft segments from the hard phase due to the stronger self-interaction of hard segments at larger NCO/OH ratio [61]. The increase in the T_g of the soft phase with increasing NCO/OH ratio and the decrease that of the hard phase in the opposite direction are the result of the partial solubility of the components and the interaction of unlike segments as predicted by the model calculations. The shape of the correlations is the same for both types of polymers, but the T_g of the two phases move closer towards each other in the polyester polyurethane compared to the polyether polymer. This shift in the transition temperatures is a clear indication of stronger interactions of unlike segments. The intensity of the transition (height of the $\text{tg } \delta$ peak in the DMA traces) of the soft phase is plotted against the NCO/OH ratio in [Fig. 3](#). Intensities are quite similar especially in the range of $-\text{OH}$ excess, but less soft segments seem to participate in the transition in the polyester polymer at large NCO content. The presence of smaller amount of relaxing soft segments is quite difficult to explain. Considering also the changes in the transition temperature of the hard phase, we must assume that more soft segments dissolve in the hard phase resulting in smaller intensity of soft phase

transition and lower hard phase T_g in the polyester than in the polyether PU, which is a further proof for stronger interactions in the former case (see [Table 3](#)).

4.3. Structure

The molecular weight of the two polyols used was nominally the same. Nevertheless, the size of the polymer molecules may be different because of the dissimilar reactivity of the polyols or kinetic effects resulting from the reaction conditions. The reaction can be followed and changes in molecular weight estimated by the measurement of torque (viscosity) in the internal mixer. Equilibrium torque is plotted against the NCO/OH ratio in [Fig. 4](#). The correlation shows a steep decrease of molecular weight with increasing deviation from equimolar stoichiometry as expected. A light asymmetry is also observed, viscosity is larger on the side of NCO excess. However, we may assume that differences in the properties of polyurethanes prepared from polyether and polyester polyols, if there are any, are not caused by dissimilarity in molecular weight. Similarly, the phase separation kinetics of the two types of polymers cannot be influenced by the size of the molecules, but by interactions.

Earlier studies proved that the phase structure of segmented linear polyurethanes consists of structural units covering several length scales [30–33]. XRD detects ordered units in the nanometer scale, SAXS offers information in the 10 nm range, while AFM and light transmittance from 20 to several 100 nm. The structure is hierarchical, smaller units organize into larger entities of various shapes and sizes [32]. The XRD patterns of selected polymers are presented in [Fig. 5](#). All the patterns are included into the [Supporting information](#) (Figs. S7 and S8). We selected samples with similar stoichiometric ratio in the entire NCO/OH range for comparison. The patterns are very similar. A definite order can be detected at the extremes of the NCO/OH range and the polymers are practically completely amorphous at equimolar stoichiometry. The pattern of the polymers prepared from the two polyols

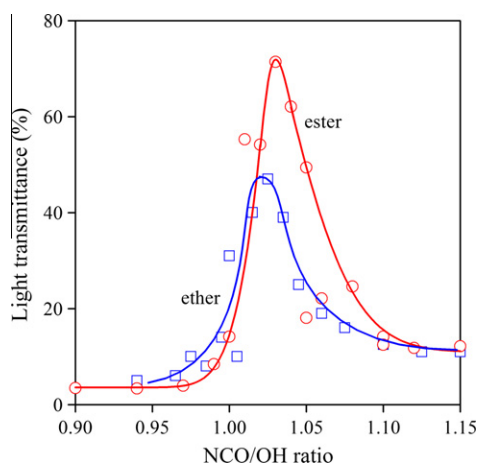


Fig. 7. Changes in the transparency of the polymers as a function of stoichiometry and type of polyol; (○) polyester, (□) polyether PU.

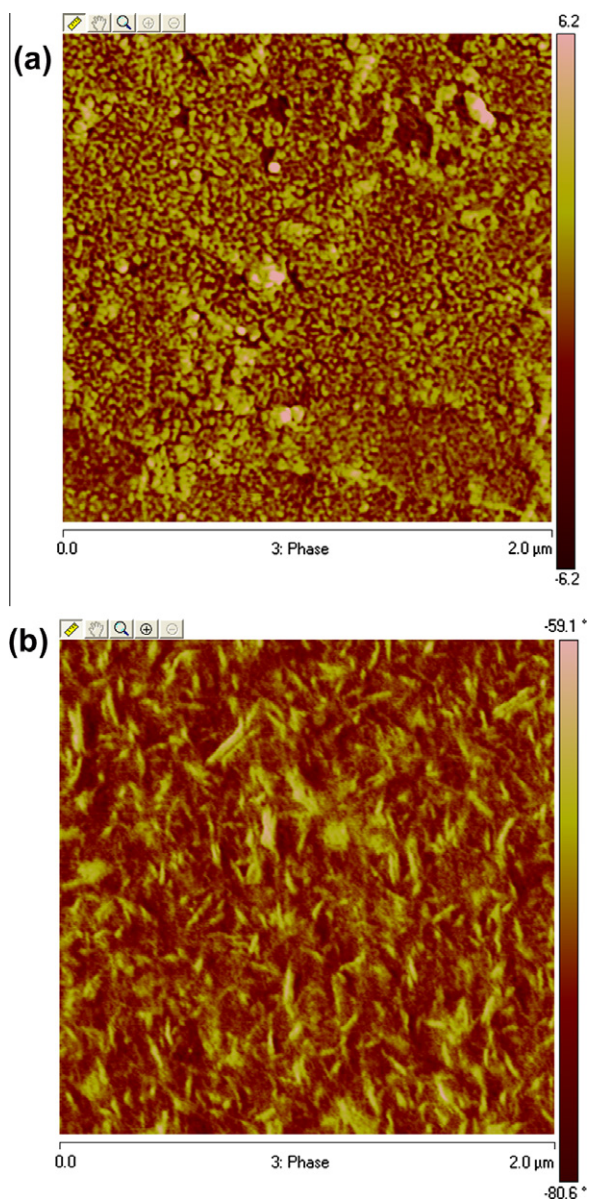


Fig. 8. AFM micrographs (phase image) taken from PU samples prepared from polyester (a) and polyether (b) polyol at the NCO/OH ratio of 1.030 and 1.025, respectively.

differs from each other at $-OH$ excess (compare the two traces at the bottom), the one recorded on the polyester polyol showing two distinct peaks. Comparison to the XRD pattern of the polyol itself and the analysis of all results proved that soft segments crystallize in the polyester PU, while they are completely amorphous in the polyether polymer. We estimated the amount of the ordered phases quantitatively by using the robust curve fitting method of Brückner [62] combined with the evaluation of Lima [53]. The order is very low, the crystallinity of the soft phase is estimated as 1–2%, but the crystallinity of the hard phase does not exceed 5% either. Although it is not obvious from Fig. 5, but crystallinity is smaller in the polyester PU at

around equimolar stoichiometry, while slightly larger at NCO excess than in the polyether PU.

SAXS patterns (Supporting information, S9 and S10) clearly indicate the existence of structural units in the 10 nm range. We plotted the position of the Bragg scattering peak (q) observed in the SAXS traces as a function of the NCO/OH ratio in Fig. 6. The position of the Bragg peak indicates that structural units scattering in this range are farther from each other in the PU prepared from the polyester polyol than in the polyether PU. Since we do not know the amount of the scattering, probably hard phase units, we can only speculate that either the number, or the size and amount of the dispersed phase particles are smaller in the polyester than in the polyether PU. This indicates slightly different phase separation kinetics and structure. Light transmission also depends on the dispersed structure of the polymer. Decreased transparency indicates the presence of particles with radii between 20 and 250 nm. Light transmission is plotted against the NCO/OH ratio in Fig. 7. A maximum is seen in the graph with larger difference between the two sets of polymers slightly above equimolar stoichiometry. The polyester PU is more transparent in this region indicating the presence of dispersed particles with smaller size or number, which agrees well with the results of XRD and SAXS studies showing less order and smaller number and/or size of the units in this range. This conclusion is strongly supported by the AFM micrographs presented in Fig. 8. At around the stoichiometric ratio of 1 a more homogeneous structure and a larger number of smaller entities can be seen in the polyester (Fig. 8a) than in the polyether polyurethane (Fig. 8b). The different chemical structure of the polyol does not change the composition dependence of structure, but definitely influences the size and probably also the arrangement of the structural units.

4.4. Properties

The tensile modulus of the two series of polymers is plotted against the stoichiometric ratio of the components

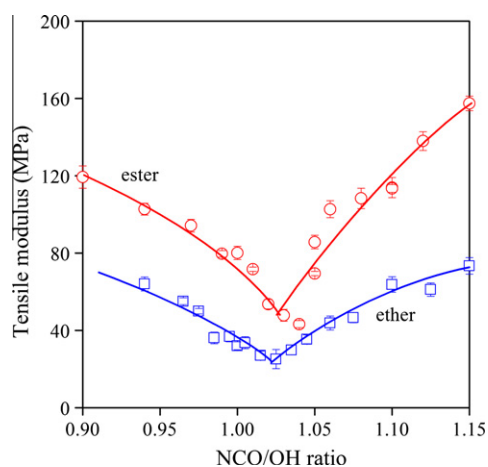


Fig. 9. Effect of stoichiometry and the type of polyol on the stiffness of polyurethane elastomers; (○) polyester, (□) polyether PU.

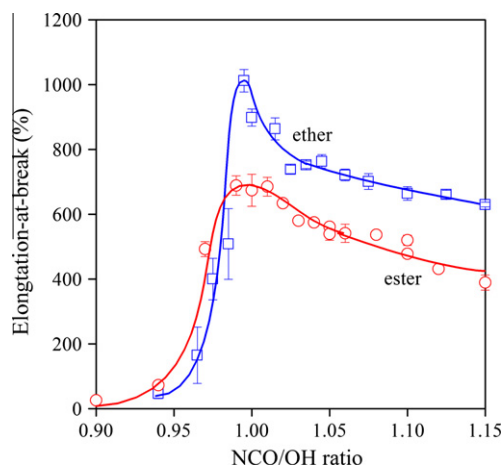


Fig. 10. Dependence of the deformability of linear polyurethanes on the NCO/OH ratio of the reaction mixture; (○) polyester, (□) polyether PU.

in Fig. 9. Stiffness goes through a minimum in both cases, but it is considerably larger for the polyester polyurethane than for its polyether counterpart. Already the minimum is difficult to explain, since changing stoichiometric ratio modifies the relative amount of hard and soft segments only slightly. Hardness and stiffness are usually adjusted by changing the polyol/total OH ratio in practice, which is kept constant here. Since the molecular weight and composition of the polymers is similar, the only difference leading to dissimilar stiffnesses is the chemical structure of the polyol, which resulted in dissimilar interactions and phase structure as shown above. Stronger hard–soft interaction in the polyester polyol resulted in increased solubility of soft segments in the hard phase and in larger overall stiffness. The minimum must be related to the smaller amount of ordered phase around stoichiometric composition as shown by the XRD measurements (see Fig. 5).

The dependence of deformability, the elongation-at-break of the samples on the composition of the reaction mixture is shown in Fig. 10. The change of tensile strength is very similar to that of elongation, except the maximum is not as sharp and the ester PU is stronger than polymers prepared with the polyether polyol. The composition dependence of the two properties (strength and elongation) is practically the same. Ultimate properties depend on the NCO/OH ratio completely differently as stiffness. The correlation is asymmetric and presents a maximum instead of a minimum. The differences are consistent and must depend on structure. Although interactions and phase structure determine both properties, an additional factor must exist which leads to the asymmetric dependence of ultimate properties on stoichiometry.

4.5. Discussion, consequences

We established in previous sections that hard–soft interactions dominate in the polyurethanes studied and these are stronger in PUs prepared with polyester than polyether polyols. The influence of interactions on phase

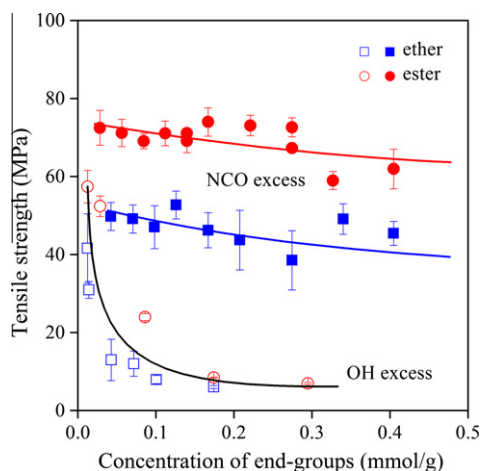


Fig. 11. Correlation between the concentration of end-groups and the strength of the linear PU elastomers studied; polyester PU –OH (○) and –NCO (●) excess, polyether PU –OH (□) and –NCO (■) excess.

structure could be proved unambiguously. The larger relative enthalpy of hard–soft interactions results in better solubility (Fig. 2), larger homogeneity (Figs. 7 and 8), smaller dispersed particles (Figs. 6 and 7) with corresponding changes in properties (Figs. 9 and 10). However, the dissimilar interactions developing in the two types of polymers do not explain the completely different dependence of stiffness and ultimate properties on the stoichiometric ratio of the functional groups and do not identify the factors determining those properties.

Earlier we showed for polyether polyurethanes that stiffness depends mainly on the amount of relaxing soft phase [63]. At the very small deformations at which stiffness is measured mainly the relative amount of the phases determines properties. Stiffness decreases with increasing amount of soft phase also in the present case. The larger

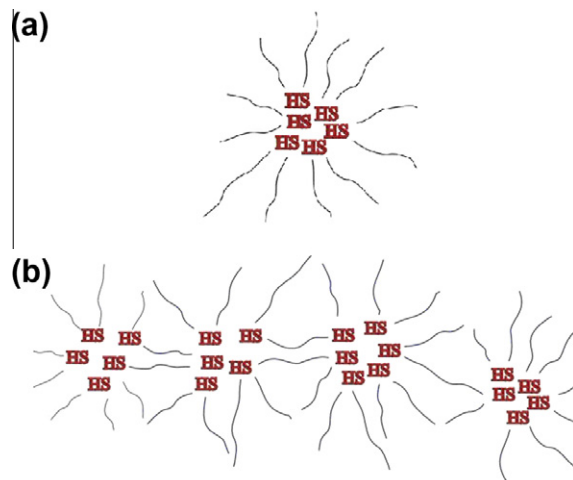


Fig. 12. Schematic representation of physical cross-links forming in the segmented polyurethanes studied at (a) –OH and (b) –NCO excess, respectively.

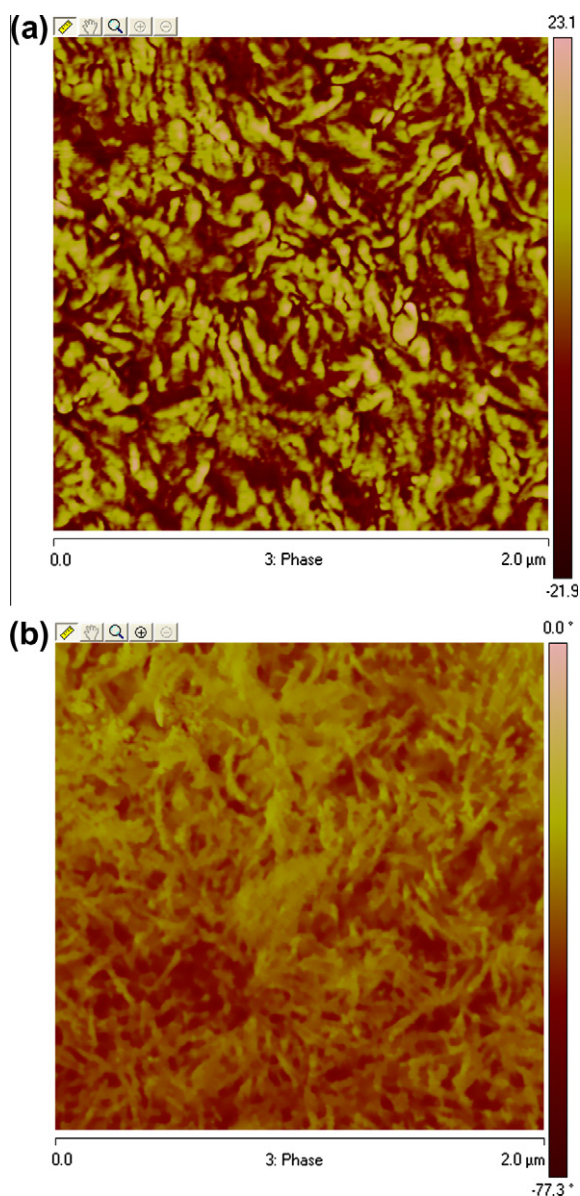


Fig. 13. Comparison of the structure of polyurethanes prepared from polyester (a) and polyether (b) polyol, respectively, at $-NCO$ excess. The stoichiometric ratio is 1.15 for both samples.

solubility of soft segments in the hard phase decreases the amount of soft phase that leads to larger stiffness for the polyester PU and modulus changes also with stoichiometry due to changing phase structure. On the other hand, ultimate properties are determined at considerably larger deformations exceeding 1000% in some cases. Fig. 11 shows the dependence of tensile strength on the concentration of end-groups. At $-OH$ excess strength decreases sharply with increasing number of end-groups. The dominating factor here is the molecular weight of the polymer which decreases drastically with increasing deviation from equimolar stoichiometry. On the other hand, strength is

much larger at NCO excess due to the interaction of the aromatic end groups which can be incorporated into the structural entities of the hard phase and even into the ordered regions detected by XRD. A schematic model of the structures formed is shown in Fig. 12. The difference in the strength of polyether and polyester PU is caused by the dissimilar number and size of the formed hard phase units acting as physical cross-links and in their properties determined by interactions. Obviously the size of these units is smaller in the polymer prepared with the polyester polyol (Figs. 6 and 7), but their number is slightly larger leading to larger strength, but smaller deformation. AFM supplies further proof for this hypothesis (Fig. 13). The PU prepared from the polyester polyol contains a larger number of well defined structural units at NCO excess (Fig. 13a) than the polyether polyurethane (Fig. 13b). The structure of the latter seems to be more diffuse with less well defined interfaces and larger interconnected structural entities. The results clearly show that besides the solubility of the phases, which is controlled by interactions, also the formation of physical cross-links play an important role in the determination of ultimate properties. The number of these latter depends on stoichiometry.

5. Conclusions

Advanced molecular modeling proved that not hard-hard, but hard-soft interactions control the phase separation of linear segmented polyurethanes. Fifteen different specific interactions were identified in polyester while thirteen in polyether PU considering only hydrogen bonds. Estimated binding enthalpy changes between 11 and 26 kJ/mol. A model was introduced to quantify the relative importance of specific interactions acting between the two types of segments. The calculations predicted better solubility of the soft phase in polyester than in polyether polyurethanes. Besides the solubility of the phases, their size and properties also depend on these interactions shown by the study of phase structure by various methods in a wide length scale. Properties are determined by different aspects of morphology. Transparency depends on the amount of ordered hard phase, stiffness and hardness on phase composition, while ultimate properties on stoichiometry, which determines molecular weight and the formation of physical cross-links.

Acknowledgements

The authors are indebted to Judith Mihály and Gábor Keresztury for their help in the recording and evaluation of FTIR-ATR spectra. András Wacha, Attila Bóta (SAXS) and István Sajó (XRD) are acknowledged for their assistance in the measurement and evaluation of the X-ray diffraction patterns. The project was partially financed by the National Scientific Research Fund of Hungary (OTKA Grant No. K 68748 and K 101124), and by the NKTH-A*STAR Hungarian-Singaporean Bilateral S&T International Co-operation (BIOSPONA); their support is highly appreciated. Mihály Kállay acknowledges the financial support provided by the European Research Council (ERC) under the

Seventh Framework Programme of EU (FP7/2007–2013), ERC Grant Agreement No. 200639, and by the Hungarian Scientific Research Fund (OTKA), Grant No. NF72194.

Appendix A. Supplementary data

Supplementary data associated with this article can be found, in the online version, at <http://dx.doi.org/10.1016/j.eurpolymj.2012.07.016>.

References

- [1] Eceiza A, Zabala J, Egiburu JL, Corcuera MA, Mondragon I, Pascault JP. Reaction kinetics of tolyl isocyanate with polyhexamethylene-pentamethylene carbonate diol. *Eur Polym J* 1999;35:1949–58.
- [2] Haska SB, Bayramli E, Pikel F, Özkaz S. Mechanical properties of HTPB-IPDI-based elastomers. *J Appl Polym Sci* 1997;64:2347–54.
- [3] Rueda-Larraz L, d'Arlas FB, Terçjak A, Ribes A, Mondragon I, Eceiza A. Synthesis and microstructure-mechanical property relationships of segmented polyurethanes based on a PCL-PTHF-PCL block copolymer as soft segment. *Eur Polym J* 2009;45:2096–109.
- [4] Rogulska M, Podkomieli W, Kultys A, Pikus S, Posdzik E. Studies on thermoplastic polyurethanes based on new diphenylethane-derivative diols. I. Synthesis and characterization of nonsegmented polyurethanes from HDI and MDI. *Eur Polym J* 2006;42:1786–97.
- [5] Lamba NMK, Woodhouse KA, Cooper SL. Polyurethanes in biomedical applications. Boca Raton: CRC Press; 1997.
- [6] Zdrachala RJ, Zdrachala IJ. Biomedical applications of polyurethanes: a review of past promises, present realities, and a vibrant future. *J Biomater Appl* 1999;14:67–90.
- [7] Guan J, Fujimoto KL, Sacks MS, Wagner WR. Preparation and characterization of highly porous, biodegradable polyurethane scaffolds for soft tissue applications. *Biomaterials* 2005;26:3961–71.
- [8] Zakharov AG, Krylov VV, Suchkov AA. Application of microballoon-catheters and microcoils in the endovascular treatment of cerebral aneurysms after subarachnoid haemorrhage. *Clin Neurol Neurosurg* 1997;99:50–1.
- [9] Bártolo P, Bidanda B. Bio-materials and prototyping applications in medicine. New York: Springer; 2008.
- [10] Moore AJ, Newell DW. Neurosurgery. New York: Springer; 2004.
- [11] Hurst RW, Rosenwasser RH. Interventional neuroradiology. New York: Informa Healthcare; 2008.
- [12] Severian D. Polymeric biomaterials. Boca Raton: CRC Press; 2002.
- [13] Seifalian AM. Effect of soft-segment chemistry on polyurethane biostability during in vitro fatigue loading. *Biomaterials* 2003;24:2549–57.
- [14] Martin DJ. Polydimethylsiloxane/polyether-mixed macrodiol-based polyurethane elastomers: biostability. *Biomaterials* 2000;20:1021–9.
- [15] Stokes K, McVenes R, Anderson JM. Polyurethane elastomer biostability. *J Biomater Appl* 1995;9:321–54.
- [16] Cozzens D, Ojha U, Kulkarni P, Faust R, Desai S. Long term in vitro biostability of segmented polyisobutylene-based thermoplastic polyurethanes. *J Biomed Mater Res* 2010;A95:774–82.
- [17] Guelcher SA, Gallagher KM, Didier JE, Klinedinst DB, Doctor JS, Goldstein AS, et al. Synthesis of biocompatible segmented polyurethanes from aliphatic diisocyanates and diurea diol chain extenders. *Biomaterials* 2005;1:471–84.
- [18] Eisenbach CD, Ribbe A, Günter C. Morphological studies of model polyurethane elastomers by element-specific electron microscopy. *Macromol Rapid Commun* 1994;15:395–403.
- [19] Bengtson B, Feger C, MacKnight WJ, Schneider NS. Thermal and mechanical properties of solution polymerized segmented polyurethanes with butadiene soft segments. *Polymer* 1985;26:895–900.
- [20] Schneider NS, Brunette CM, Hsu SL, MacKnight WJ. Structure and properties of polybutadiene polyurethanes. *Adv Urethane Sci Technol* 1981;8:49–74.
- [21] Brunette CM, Hsu SL, Rossman M, MacKnight WJ, Schneider NS. Thermal and mechanical properties of linear segmented polyurethanes with butadiene soft segments. *Polym Eng Sci* 1981;21:668–74.
- [22] Balabin RM, Syunyaev RZ, Schmid T, Stadler J, Lomakina EI, Zenobi R. Asphaltene adsorption onto an iron surface. Combined near infrared (NIR), Raman, and AFM study of the kinetics, thermodynamics, and layer structure. *Energy Fuels* 2010;25:189–96.
- [23] Balabin RM. Polar (acyclic) isomer of formic acid dimer: gas-phase Raman spectroscopy study and thermodynamic parameters. *J Phys Chem* 2009;A113:4910–8.
- [24] Balabin RM. Enthalpy difference between conformations of normal alkanes: Raman spectroscopy study of *n*-pentane and *n*-butane. *J Phys Chem* 2009;A113:1012–9.
- [25] Camberlin Y, Pascault JP. Phase segregation kinetics in segmented linear polyurethanes: Relations between equilibrium time and chain mobility and between equilibrium degree of segregation and interaction parameter. *J Polym Sci Polym Phys* 1984;22:1835–44.
- [26] Dobrosielska K, Takano A, Matsushita Y. Creation of hierarchical nanophase-separated structures via supramacromolecular self-assembly from two asymmetric block copolymers with short interacting sequences giving hydrogen bonding interaction. *Macromolecules* 2009;43(2):1101–7.
- [27] Bras W, Derbyshire GE, Bogg D, Cooke J, Elwell MJ, Komanshek BU, et al. Simultaneous studies of reaction kinetics and structure development in polymer processing science. *Science* 1995;267:996–9.
- [28] Yilgör E, Burgaz E, Yurtsever E, Yilgör I. Comparison of hydrogen bonding in polydimethylsiloxane and polyether based urethane and urea copolymers. *Polymer* 2000;41:849–57.
- [29] Zhang C, Hu J, Chen S, Ji F. Theoretical study of hydrogen bonding interactions on MDI-based polyurethane. *J Mol Model* 2010;16:1391–9.
- [30] Tocha E, Janik H, Debowski H, Vancso GJ. Morphology of polyurethanes revisited by complementary AFM and TEM. *J Macromol Sci Phys* 2002;B41:1291–304.
- [31] Chu B, Gao T, Li Y, Wang J, Desper CR, Byrne CA. Microphase separation kinetics in segmented polyurethanes: effects of soft segment length and structure. *Macromolecules* 1992;25:5724–9.
- [32] Xu M, MacKnight WJ, Chen-Tsai CHY, Thomas EL. Structure and morphology of segmented polyurethanes: 4. Domain structures of different scales and the composition heterogeneity of the polymers. *Polymer* 1987;28:2183–9.
- [33] Li Y, Liu J, Yang H, Ma D, Chu B. Multiphase structure of segmented polyurethanes: Its relation with spherulite structure. *J Polym Sci Polym Phys* 1993;31:853–67.
- [34] Crawford DM, Bass RG, Haas TW. Strain effects on thermal transitions and mechanical properties of thermoplastic polyurethane elastomers. *Thermochim Acta* 1998;323:53–63.
- [35] Chang CC, Chen KS, Yu TL, Chen YS, Tsai CL, Tseng YH. Phase segregation of polyester based polyurethanes. *Polym J* 1999;31:1205–10.
- [36] Chen WP, Schlick S. Study of phase separation in polyurethanes using paramagnetic labels: effect of soft-segment molecular weight and temperature. *Polymer* 1990;31:308–14.
- [37] Kojio K, Nakashima S, Furukawa M. Microphase-separated structure and mechanical properties of norbornane diisocyanate-based polyurethanes. *Polymer* 2007;48:997–1004.
- [38] Seymour RW, Estes GM, Cooper SL. Infrared studies of segmented polyurethane elastomers. I. Hydrogen bonding. *Macromolecules* 1970;3:579–83.
- [39] Monteiro EEC, Fonseca JLC. Stress relaxation of thermoplastic polyurethanes monitored by FTIR spectroscopy. *Polym Test* 1999;18:281–6.
- [40] Yilgör I, Mather BD, Unal S, Yilgör E, Long TE. Preparation of segmented, high molecular weight, aliphatic poly(ether-urea) copolymers in isopropanol. In-situ FTIR studies and polymer synthesis. *Polymer* 2004;45:5829–36.
- [41] Briber RM, Thomas EL. The structure of MDI/BDO-based polyurethanes: Diffraction studies on model compounds and oriented thin films. *J Polym Sci Polym Phys* 1985;23:1915–32.
- [42] Blackwell J, Gardner KH. Structure-property relationships of poly(urethane urea)s with ultra-low monol content poly(propylene glycol) soft segments. I. Influence of soft segment molecular weight and hard segment content. *Polymer* 1979;20:13–7.
- [43] O'Sickey MJ, Lawrey BD, Wilkes GL. Structure-property relationships of poly(urethane urea)s with ultra-low monool content poly(propylene glycol) soft segments I. Influence of soft segment molecular weight and hard segment content. *J Appl Polym Sci* 2002;84:229–43.
- [44] Koberstein JT, Russell TP. Simultaneous SAXS-DSC study of multiple endothermic behavior in polyether-based polyurethane block copolymers. *Macromolecules* 1986;19:714–20.
- [45] Koberstein JT, Stein RS. Small-angle light scattering studies of macro-phase separation in segmented polyurethane block copolymers. *Polymer* 1984;25:171–7.

- [46] Eisenbach CD, Ribbe A, Günter C. Morphological studies of model polyurethane elastomers by element-specific electron microscopy. *Macromol Rapid Commun* 1994;15:395–403.
- [47] Sonnenschein MF, Lysenko Z, Brune DA, Wendt BL, Schrock AK. Enhancing polyurethane properties via soft segment crystallization. *Polymer* 2005;46:10158–66.
- [48] Magonov SN, Reneker DH. Characterization of polymer surfaces with atomic force microscopy. *Ann Rev Mater Sci* 1997;27:175–222.
- [49] Christenson EM, Anderson JM, Hiltner A, Baer E. Relationship between nanoscale deformation processes and elastic behavior of polyurethane elastomers. *Polymer* 2005;46:11744–54.
- [50] Ginzburg VV, Bicerano J, Christenson CP, Schrock AK, Patashinski AZ. Theoretical modeling of the relationship between Young's modulus and formulation variables for segmented polyurethanes. *J Polym Sci Polym Phys* 2007;45:2123–35.
- [51] Stangret J, Kamienska-Piotrowicz E, Laskowska K. FT-IR studies of molecular interactions in formamide-methanol mixtures. *Vibr Spectr* 2007;44:324–30.
- [52] Zhao Y, Truhlar DG. Hybrid meta density functional theory methods for thermochemistry, thermochemical kinetics, and noncovalent interactions: The MPW1B95 and MPWB1K models and comparative assessments for hydrogen bonding and van der Waals interactions. *J Phys Chem* 2004;A108:6908–18.
- [53] Krishnan R, Binkley JS, Seeger R, Pople JA. Self-consistent molecular orbital methods. XX. A basis set for correlated wave functions. *J Chem Phys* 1980;72:650–4.
- [54] Zhang RB, Somers KRF, Kryachko ES, Nguyen MT, Zeegers-Huykens T, Ceulemans A. Hydrogen bonding to π -systems of indole and 1-methylindole: is there any OH...Phenyl bond. *J Phys Chem* 2005;A109:8028–34.
- [55] Balabin RM. Enthalpy difference between conformations of normal alkanes: Effects of basis set and chain length on intramolecular basis set superposition error (BSSE). *Mol Phys* 2011;109:943–53.
- [56] Balabin RM. Enthalpy difference between conformations of normal alkanes: Intramolecular basis set superposition error (BSSE) in the case of n-butane and n-hexane. *J Chem Phys* 2008;129:164101.
- [57] Frisch MJ, et al. Gaussian 03, Revision B.01. Gaussian Inc., Pittsburgh PA, 2003.
- [58] Flory JP. Principles of polymer chemistry. Ithaca: Cornell University; 1953.
- [59] Lohse DJ, Graessley WW. Thermodynamics of polyolefin blends. In: Paul DR, Bucknall CB, editors. *Editors*. New York: Wiley; 2000. p. 219–37.
- [60] Olabisi O, Robson LM, Shaw MT. Polymer-polymer miscibility. New York: Academic; 1979. p. 104.
- [61] Pukánszky Jr B, Bagdi K, Tóvölgyi Z, Varga J, Botz L, Hudak S, et al. Nanophase separation in segmented polyurethane elastomers: Effect of specific interactions on structure and properties. *Eur Polym J* 2008;44(8):2431–8.
- [62] Brückner S. Estimation of the background in powder diffraction patterns through a robust smoothing procedure. *J Appl Cryst* 2000;33:977–9.
- [63] Bagdi K, Molnár K, Pukánszky BJ, Pukánszky B. Thermal analysis of the structure of segmented polyurethane elastomers. *J Therm Anal Calor* 2009;98(3):825–32.